High sensitivity of BRCA1-deficient mammary tumors to the PARP inhibitor AZD2281 alone and in combination with platinum drugs

Sven Rottenberg[a], Janneke E. Jaspers[a], Ariena Kersbergen[a], Eline van der Burg[a], Anders O. H. Nygren[b], Serge A. L. Zander[a], Patrick W. B. Derksen[a,1], Michiel de Bruin[a], John Zevenhoven[c], Alan Lau[d], Robert Boulter[d], Aaron Cranston[d], Mark J. O'Connor[d], Niall M. B. Martin[d], Piet Borst[a], and Jos Jonkers[a,2]

[a]Division of Molecular Biology and Centre for Biomedical Genetics and [c]Division of Molecular Genetics, The Netherlands Cancer Institute, Plesmanlaan 121, 1066 CX Amsterdam, The Netherlands; [b]MRC–Holland, Willem Schoutenstraat 6, 1057 DN Amsterdam, The Netherlands; and [d]KuDOS Pharmaceuticals, Ltd., 410 Cambridge Science Park, Milton Road, Cambridge, CB4 0PE, United Kingdom

Edited by Harold E. Varmus, Memorial Sloan–Kettering Cancer Center, New York, NY, and approved August 25, 2008 (received for review June 25, 2008)

Whereas target-specific drugs are available for treating ERBB2-overexpressing and hormone receptor-positive breast cancers, no tailored therapy exists for hormone receptor- and ERBB2-negative ("triple-negative") mammary carcinomas. Triple-negative tumors account for 15% of all breast cancers and frequently harbor defects in DNA double-strand break repair through homologous recombination (HR), such as BRCA1 dysfunction. The DNA-repair defects characteristic of BRCA1-deficient cells confer sensitivity to poly-(ADP-ribose) polymerase 1 (PARP1) inhibition, which could be relevant to treatment of triple-negative tumors. To evaluate PARP1 inhibition in a realistic in vivo setting, we tested the PARP inhibitor AZD2281 in a genetically engineered mouse model (GEMM) for BRCA1-associated breast cancer. Treatment of tumor-bearing mice with AZD2281 inhibited tumor growth without signs of toxicity, resulting in strongly increased survival. Long-term treatment with AZD2281 in this model did result in the development of drug resistance, caused by up-regulation of *Abcb1a/b* genes encoding P-glycoprotein efflux pumps. This resistance to AZD2281 could be reversed by coadministration of the P-glycoprotein inhibitor tariquidar. Combination of AZD2281 with cisplatin or carboplatin increased the recurrence-free and overall survival, suggesting that AZD2281 potentiates the effect of these DNA-damaging agents. Our results demonstrate in vivo efficacy of AZD2281 against BRCA1-deficient breast cancer and illustrate how GEMMs of cancer can be used for preclinical evaluation of novel therapeutics and for testing ways to overcome or circumvent therapy resistance.

breast cancer | drug resistance | P-glycoprotein | GEMM | DNA repair

Poly(ADP-ribose) polymerase 1 (PARP1) is involved in surveillance and maintenance of genome integrity and functions as a key molecule in the repair of DNA single-strand breaks (SSBs) (1–3). Inactivation of SSB repair by PARP1 inhibition during S-phase induces DNA double-strand breaks (DSBs) and may thus confer synthetic lethality to cells with defective homology-directed DSB repair (4, 5). Mutations in *BRCA1* or *BRCA2* predispose to hereditary breast and ovarian cancer, which accounts for 3–5% of all breast cancers and a greater proportion of ovarian cancers (6). BRCA1 and BRCA2 function is critical for homologous recombination (HR) (6, 7), and BRCA-deficient cells appear to be highly sensitive to PARP inhibition, resulting in increased genomic instability, cell cycle arrest, and apoptosis (4, 5). PARP1 inhibition might, therefore, be a specific therapy for cancers with defects in *BRCA1/2* or other HR pathway components (clinically relevant PARP inhibitors are reviewed in ref. 8). Recently, Donawho *et al.* (9) have reported that the PARP inhibitor ABT-888 in combination with platinum drugs or cyclophosphamide, but not alone, causes regression of BRCA1-deficient MX-1 xenografts. However, this study uses only a single *BRCA1*-mutated tumor line without isogenic controls to address the impact of *BRCA1* mutation on response to PARP inhibition. In addition, xenografts in immunodeficient mice do not sufficiently mimic the tumor–host interactions of real breast cancers in women (10). To assess the therapeutic potential of PARP1 inhibition in a more realistic BRCA1-deficient mammary tumor model, we tested the PARP inhibitor AZD2281 (11) in our *K14cre;Brca1$^{F/F}$;p53$^{F/F}$* mouse model for hereditary breast cancer. The *Brca1$^{-/-}$;p53$^{-/-}$* mammary adenocarcinomas arising in this model recapitulate several key features of human BRCA1-associated breast cancer, including a basal-like phenotype, lack of ER-, PR-, and ERBB2-expression and a high degree of genomic instability (12) and may therefore be a good predictor for clinical responses of BRCA1-deficient cancers to AZD2281.

Results

***Brca1$^{-/-}$;p53$^{-/-}$* Mammary Tumors Respond to the PARP Inhibitor AZD2281.** An important feature of the spontaneous *Brca1$^{-/-}$;p53$^{-/-}$* mammary tumors in the *K14cre;Brca1$^{F/F}$;p53$^{F/F}$* mouse model is that they can be transplanted orthotopically into wild-type female mice without losing their basal-like phenotype, gene expression profile, or sensitivity to anticancer agents (13). Fig. 1 illustrates how this orthotopic transplantation system was used to test various treatment regimens of AZD2281 as single agent or in combination therapy on genetically identical tumors. We first determined the PARP inhibitory dose of AZD2281 in tumor-bearing mice. As shown in Fig. 2*A*, AZD2281 given at 50 mg/kg per day is rapidly taken up by the tumor but is also quickly cleared. However, compared with the plasma concentration (data not shown), the intratumoral levels of AZD2281 were ≈2- and 6- to 8-fold higher at 2 and 6 h after injection, respectively, suggesting tumor loading of AZD2281. Importantly, we observed a reduction of the intratumoral PARP1 activity to ≈25% of predose levels 30 min after treatment, which returned back to 77% after 24 h (Fig. 2*A*).

Next, we treated animals harboring 9 individual *Brca1$^{-/-}$;*

Author contributions: S.R., M.J.O., N.M.B.M, P.B., and J.J. designed research; S.R., J.E.J., A.K., E.v.d.B., A.O.H.N., S.A.L.Z., P.W.B.D., M.d.B., J.Z., A.L., R.B., and A.C. performed research; S.R., J.E.J., A.K., E.v.d.B., A.O.H.N., A.L., R.B., A.C., M.J.O., N.M.B.M, P.B., and J.J. analyzed data; and S.R., P.B., and J.J. wrote the paper.

Conflict of interest statement: A.O.H.N. is an employee of MRC-Holland BV, which markets the MLPA test used in this article. A.L., R.B., A.C., M.J.O., and N.M.B.M. are employees of KuDOS Pharmaceuticals, which developed AZD2281.

This article is a PNAS Direct Submission.

Freely available online through the PNAS open access option.

[1]Present address: Department of Medical Oncology, Heidelberglaan 100, 3584 CX, University Medical Center Utrecht, Utrecht, The Netherlands.

[2]To whom correspondence should be addressed. E-mail: j.jonkers@nki.nl.

This article contains supporting information online at www.pnas.org/cgi/content/full/0806092105/DCSupplemental.

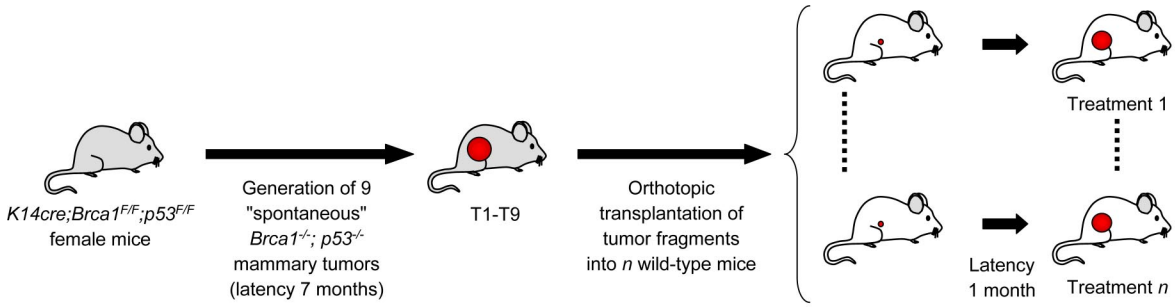

Tumor \ Treatment	PK/PD	Untreated	Vehicle	PARPi 28-d	PARPi 28-d + tariquidar	PARPi 100-d	Cisplatin	Cisplatin + PARPi 28-d	Cisplatin + PARPi 100-d	Carboplatin	Carboplatin + PARPi 28-d	Carboplatin + PARPi 100-d
T1	●	●	●	●	●	●	●	●	●	●	●	
T2	●	●	●	●	●	●	●	●	●	●	●	●
T3	●	●	●	●	●	●	●	●	●	●	●	●
T4		●	●	●	●	●	●	●	●	●	●	●
T5		●	●	●		●	●	●	●	●	●	●
T6		●		●	●	●	●	●	●	●	●	
T7		●		●		●	●	●	●	●	●	●
T8		●		●			●	●		●	●	
T9		●		●			●	●		●		

Fig. 1. Overview of tumor transplantations and drug treatments in this study. Small tumor fragments of 9 spontaneous mammary tumors (T1–T9), which developed in *K14cre;Brca1$^{F/F}$;p53$^{F/F}$* mice (Liu *et al.*, ref. 12) were transplanted orthotopically into syngeneic wild-type female mice. After a mean latency of ≈4 weeks, when tumors reached a size of 150–250 mm^3 (V = length × width^2 × 0.5), the indicated drug treatments were carried out. Dosing was as follows: 50 mg of AZD2281 per kg i.p. daily for 28 days (28 days) or daily for 100 days (100 days), 6 mg of cisplatin per kg i.v. on day 0 (30 min after the first AZD2281 injection), 100 mg of carboplatin per kg i.v. on day 0 (30 min after the first AZD2281 injection), 2 mg of tariquidar per kg every other day (if combined with AZD2281, tariquidar was given 30 min in advance). Treatment of tumors was resumed once the tumor relapsed to its original size (100%).

p53$^{-/-}$ tumors (T1–T9) with AZD2281 (50 mg/kg i.p. per day) for 28 consecutive days once the tumor volume was between 150 and 250 mm^3 (Fig. 2*C*). Compared with untreated (Fig. 2*B*) and vehicle-treated controls [supporting information (SI) Fig. S1], all tumors responded to AZD2281. After a lag time of ≈5 days, T1–T7 stopped growing and showed a substantial shrinkage ranging from nonpalpable to a nodule of ≈40% of the initial size. As additional control for the selective targeting of HR-deficient cells by AZD2281, we treated 5 individual *Ecad*$^{-/-}$*;p53*$^{-/-}$ tumors from a mouse model for pleomorphic invasive lobular carcinoma (ref. 14 and P.W.B.D. and J.J., unpublished results). None of these HR-proficient tumors responded to AZD2281 (Fig. S2). The lag phase we observed in *Brca1*$^{-/-}$*;p53*$^{-/-}$ tumors might be explained by the fact that PARP1 inhibition is not cytotoxic by itself but acts by forcing BRCA1-deficient cells to employ error-prone repair pathways that eventually result in cell death (5). This notion is supported by our finding that DNA damage-associated γH2AX foci and cleaved caspase 3-positive cells are significantly increased after 7 days of daily AZD2281 treatment compared with untreated *Brca1*$^{-/-}$*;p53*$^{-/-}$ tumors or AZD2281-treated HR-proficient *Ecad*$^{-/-}$*;p53*$^{-/-}$ mammary tumors (Fig. 3 and Table S1). After withdrawal of treatment, tumors began to grow again with various lag times (Fig. 2*C*), and when tumors reached 100% of the original volume at the time of treatment initiation, a second course of AZD2281 (50 mg/kg i.p. per day ×28) was administered. The relapsing tumors, however, did not respond to AZD2281 treatment at this point and lacked the increased numbers of γH2AX and cleaved caspase 3-positive

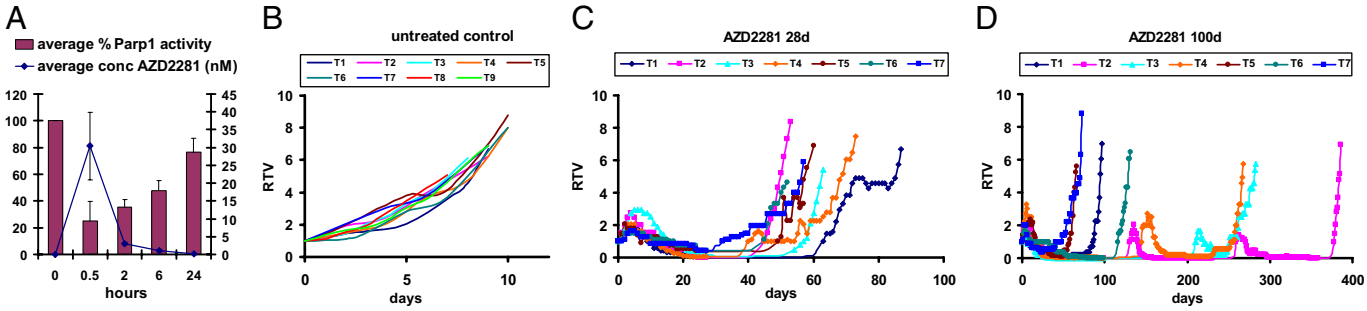

Fig. 2. Treatment of mice carrying orthotopically transplanted *Brca1*$^{-/-}$*;p53*$^{-/-}$ tumors with 50 mg of AZD2281 per kg i.p. (*A*) Intratumoral concentration of AZD2281 and PARP1 activity over time. Error bars indicate SEM. (*B–D*) Animals carrying 9 individually transplanted tumors (T1–T9) were either left untreated, or received AZD2281 daily for 28 or 100 days. Graphs show relative tumor volume (RTV, ratio of tumor volume to initial size at start of treatment) as a function of time. T8 and T9 showed stable disease and received continuous dosing beyond the 28 days (see Fig. S1). Once the tumors relapsed, treatment was resumed when the tumor size reached 100% of the original volume. Days on which AZD2281 was given are indicated by circles, triangles, or squares.

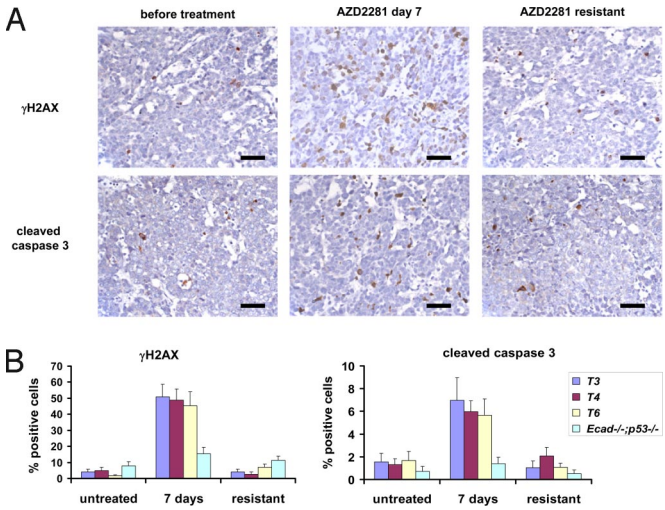

Fig. 3. AZD2281 treatment induces DNA damage-associated foci and caspase 3-mediated apoptosis. (*A*) Example of the IHC analysis of T4 using anti-activated caspase 3 and anti-γH2AX-specific antibodies. Sections of the sensitive tumor (before or 7 days after daily injection of 50 mg of AZD2281 per kg i.p.) and resistant tumor (day 73 after unsuccessful daily treatment of the relapsing tumor, see Fig. 2*C*) are shown. Bar = 50 μm. (*B*) Quantification of γH2AX or cleaved caspase 3-positive cells of 3 individual $Brca1^{-/-};p53^{-/-}$ tumors (T3, T4, T6) and $Ecad^{-/-};p53^{-/-}$ tumor 1 before, 7 days after daily AZD2281 treatment or of the outgrown AZD2281-resistant tumor (see Fig. 2*C* and Fig. S2). For *P* values see Table S1.

cells detected during the first course of AZD2281 administration (Fig. 3).

Prolonged AZD2281 Treatment Increases Overall Survival Without Obvious Signs of Toxicity. In the 2 cases where mice engrafted with tumors (T8 and T9) exhibited stable disease, continuous dosing beyond 28 days was carried out with AZD2281 (Fig. S1). Eventually, these tumors also failed to respond to AZD2281. Importantly, continuous treatment for 58 (T8) and 156 days (T9) did not result in any obvious signs of toxicity such as weight loss, apathy, or pathological abnormalities at necropsy. Therefore, in an attempt to eradicate $Brca1^{-/-};p53^{-/-}$ tumors, we repeated the experiments with tumors T1–T7 but extended AZD2281 treatment to 100 days (Fig. 2*D*). Again, all tumors shrank to small or nonpalpable remnants. For tumors T1, T5, and T7, resistance was acquired during treatment, whereas T6 relapsed to 100% of the pretreatment volume on day 116 without responding to a second course of AZD2281. Notably, relapsed tumors T2, T3, and T4 were sensitive to the resumption of AZD2281 administration but developed resistance during the second (T3 and T4) or third 100-day cycle of AZD2281 (T2). Hence, compared with the 28-day dosing schedule, the 100-day schedule significantly increased the median survival of the mice from 60 to 131 days (Fig. 5*B*). Also, in animals undergoing extended AZD2281 treatment, no signs of toxicity were observed.

AZD2281 Resistance Is Frequently Caused by Increased Expression of *Abcb1a/b*. To investigate mechanisms of acquired resistance to AZD2281, which arose in all tumors investigated, we analyzed the expression levels of several drug efflux transporter genes in addition to the drug target gene *Parp1* in AZD2281-sensitive tumors and their AZD2281-resistant counterparts using reverse transcriptase-multiplex ligation-dependent probe amplification (RT-MLPA; Fig. 4*A* and Table S2). Most strikingly, the expression of the drug efflux transporters *Abcb1a* or *Abcb1b* (15), which encode the murine P-glycoproteins, was increased by 2- to 85-fold in 11 of 15 AZD2281-resistant tumors. Approximately a 2.5-fold increased expression of *Abcg2* (*Bcrp1*) (16) was observed in 3 tumors (T2–28, T3–100 and T6–100), whereas no change in the *Abcc1* or *Hprt1* expression was detected. Up-regulation of the drug target *Parp1* was found in tumors T6–28 (2.7-fold) and T6–100 (4.2-fold).

Because acquired doxorubicin resistance in the $K14cre;Brca1^{F/F};p53^{F/F}$ model is frequently caused by increased *Abcb1a* and *Abcb1b* expression (13), we studied the effects of AZD2281 on doxorubicin-resistant tumors with or without increased *Abcb1a/b* expression (Fig. 4*B*). Of 3 doxorubicin-resistant tumors analyzed, only those with increased *Abcb1a/b* expression showed primary resistance to AZD2281. The doxorubicin-resistant tumor without altered drug transporter expression responded initially to drug but eventually developed AZD2281 resistance, which was characterized by a 3.6-fold increase in *Abcb1b* expression. To test whether acquired AZD2281 resistance could be reversed by blocking drug transporter activity, we combined AZD2281 treatment with the specific third-generation P-glycoprotein (P-gp) inhibitor tariquidar (XR9576) (17). For this purpose, tumors T1–T4 and T6 were first treated with AZD2281 for 28 days, resulting in complete regression (Fig. 4*C*). When tumors relapsed after withdrawal of the PARP inhibitor, tariquidar was applied alone or in combination with a second cycle of AZD2281. In contrast to relapsed tumors T1–T3 and T6 treated with AZD2281 alone, tumor recurrences again became sensitive to AZD2281 by concurrent inhibition of P-gp using tariquidar. T4 showed stable disease, suggesting that other mechanisms of resistance may also evolve. Such mechanisms might explain AZD2281 resistance of T1–100, T5–28, and T4–28, which do not show marked up-regulation of drug transporter gene expression. Of note, T6 (showing marked up-regulation of *Abcb1b*) responded to P-gp inhibition using tariquidar despite an increased mRNA expression of the drug target *Parp1*, indicating that AZD2281 resistance in this tumor is primarily caused by P-gp overexpression.

Combination of AZD2281 with Platinum Drugs Increases Recurrence-Free and Overall Survival. Inhibition of PARP has also been reported to enhance the effects of DNA-damaging anticancer drugs such as temozolomide, platinums, and cyclophosphamide in BRCA1-deficient cells (9). Indeed, in vitro combination studies showed strong and selective synergy between AZD2281 and cisplatin in suppressing BRCA2-deficient mammary tumor cell growth (18). From a previous study, we know that mammary tumors in our $K14cre;Brca1^{F/F};p53^{F/F}$ model are sensitive to the MTD of cisplatin and do not acquire resistance (13). We therefore tested the combination of AZD2281 with cisplatin and carboplatin in this model according to a defined treatment schedule (see *Materials and Methods*). Compared with cisplatin or carboplatin monotherapy, combination treatment with cisplatin and 28- or 100-day cycles of AZD2281 significantly prolonged both recurrence-free survival (Fig. 5*A* and Table S3) and overall survival (Fig. 5*B* and Table S4). These results indicate that AZD2281 potentiates the effect of these platinum drugs. Nevertheless, most tumors could not be eradicated with the current AZD2281-platinum combination schedules and tended to relapse (Fig. 5*A* and Fig. S1). Moreover, we observed increased toxicity of cisplatin in combination with AZD2281. Mice tolerated an average of 6.7 cycles of cisplatin (6 mg/kg i.v., SD = 1, n = 9) before they had to be killed because of accumulating nephrotoxicity. In contrast, mice tolerated only 3 cycles of cisplatin (6 mg/kg i.v. day 0) + 100 daily injections of 50 mg of AZD2281 per kg (SD = 0.7, n = 5).

Discussion

Here, we show that the $K14cre;Brca1^{F/F};p53^{F/F}$ mouse model is useful for preclinical evaluation of novel therapeutics, such as the clinical PARP inhibitor AZD2281. We found that BRCA1-

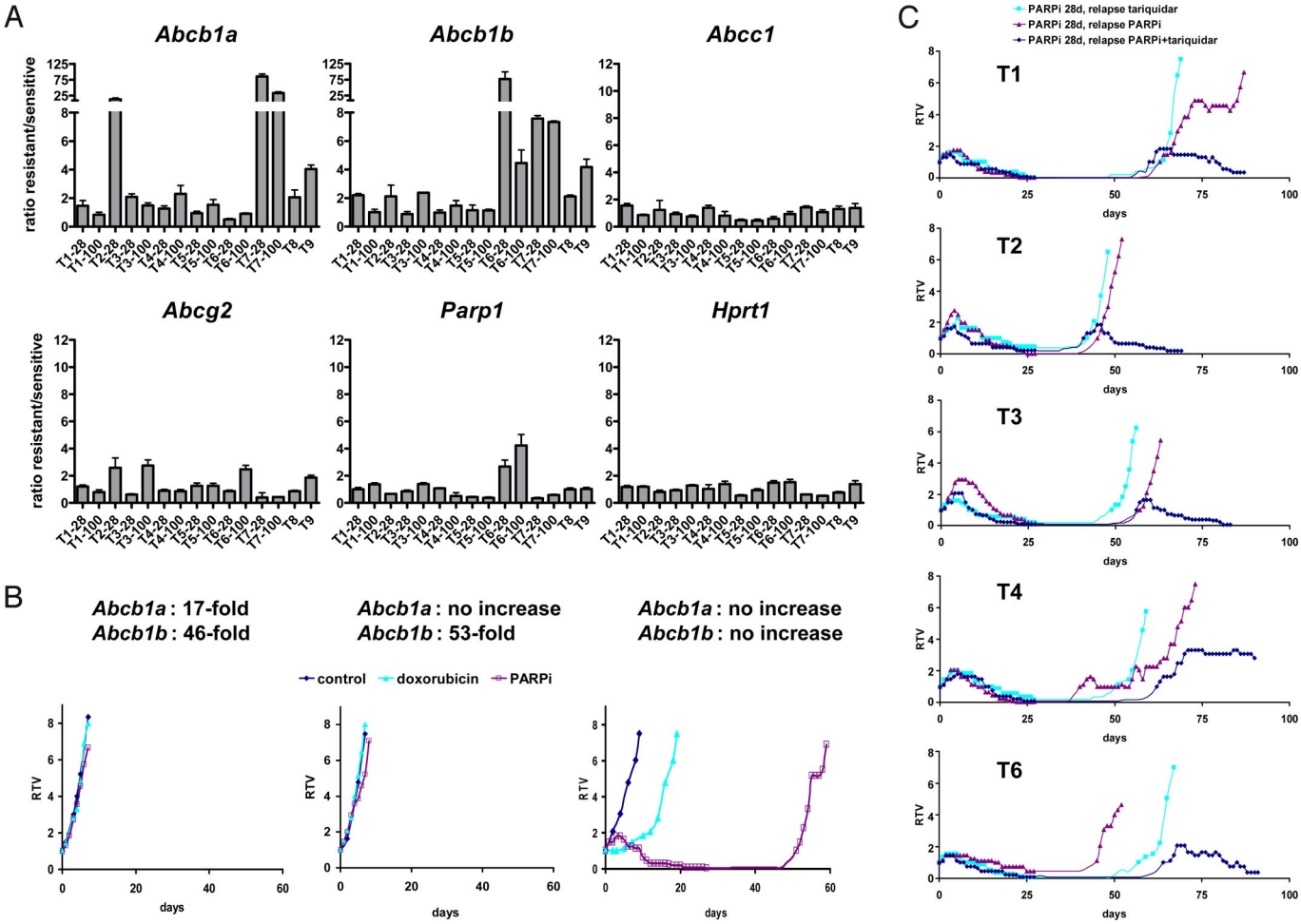

Fig. 4. Increased expression of *Abcb1a* and *Abcb1b* is associated with AZD2281 resistance in vivo. (*A*) RT-MLPA analysis of the ratios of *Abcb1a*, *Abcb1b*, *Abcc1*, *Abcg2*, *Parp1*, and *Hprt1* expression in AZD2281-resistant tumors and samples from the corresponding untreated tumors. *Actin-β* expression was used as internal reference. The values presented are the mean ratio of 3 independent reactions. The suffix 28 indicates the 28-day schedule of AZD2281 and 100 the 100-day schedule. Error bars indicate standard deviation. For the complete dataset see Table S2. (*B*) Three *Brca1*$^{-/-}$;*p53*$^{-/-}$ doxorubicin-resistant tumors (2 with up-regulation of *Abcb1a/b* and 1 without; ref. 13) were tested for their response to AZD2281. Days on which 50 mg of AZD2281 per kg were given have open squares. (*C*) T1–T4 and T6 were treated with a daily injection of 50 mg of AZD2281 per kg for 28 days. When tumors relapsed to 100% of their original volume, they were retreated by i.p. injection of 2 mg of tariquidar per kg every other day (light blue line) or 50 mg of AZD2281 per kg daily (red line) or both (dark blue line). Days on which animals were treated are indicated by rhombi, triangles, or squares. Graphs in *B* and *C* show relative tumor volume (RTV, ratio of tumor volume to initial size at start of treatment) as a function of time.

deficient "spontaneous" mouse mammary tumors show an impressive and prolonged response to AZD2281. This is consistent with the reported hypersensitivity of BRCA1-deficient cells to PARP1 inhibition (5). An important advantage of AZD2281 is its excellent therapeutic index. Even after prolonged daily treatment with a PARP1-inhibitory dose of AZD2281, no dose-limiting toxicity is observed in tumor-bearing mice. Because also BRCA2-deficient mouse mammary tumor cells demonstrate selective sensitivity to AZD2281 (18), this PARP inhibitor may represent a promising drug against BRCA-associated breast and ovarian cancer in humans. In addition, sporadic cancers with HR pathway defects may also be expected to show selective sensitivity to AZD2281. In particular, treatment of patients with triple-negative breast cancers, which account for 15% of all breast cancers (19) and frequently harbor BRCA1 pathway defects (20–23), might be useful, because no targeted therapy exists thus far for this subgroup of breast cancers. Preliminary data from Phase I clinical trials with AZD2281 also indicate a favorable toxicity profile and objective responses in several patients with BRCA1-associated ovarian cancer (24). Regarding administration of AZD2281 as a single agent, our data suggest that continuous dosing of the PARP inhibitor may be more effective than intermittent treatment. Continuous AZD2281 treatment might result in increased toxicity in nontumor cells carrying heterozygous *BRCA* mutations compared with wild-type nontumor cells, but continuous dosing of AZD2281 in *BRCA1* mutation carriers does not suggest this to be the case (24).

Genetically engineered mouse models (GEMMs) of BRCA-associated breast cancer also enable preclinical evaluation of combination treatments that increase the types of DNA damage for which repair will be abrogated after PARP1 inhibition in a BRCA-deficient genetic background. A promising therapeutic strategy involves combination treatment with PARP inhibitors and platinum drugs, which induce, in addition to interstrand cross-links, intrastrand cross-links that are removed by nucleotide-excision repair (NER) (25). Because PARP1 might be involved in both base-excision repair (BER) and NER (26), synergy between PARP inhibitors and platinum drugs could be anticipated. Indeed, in vitro drug combination studies showed selective synergy between AZD2281 and cisplatin in BRCA2-deficient mammary tumor cell lines (18). In line with this, we found that AZD2281 may enhance the efficacy of platinum

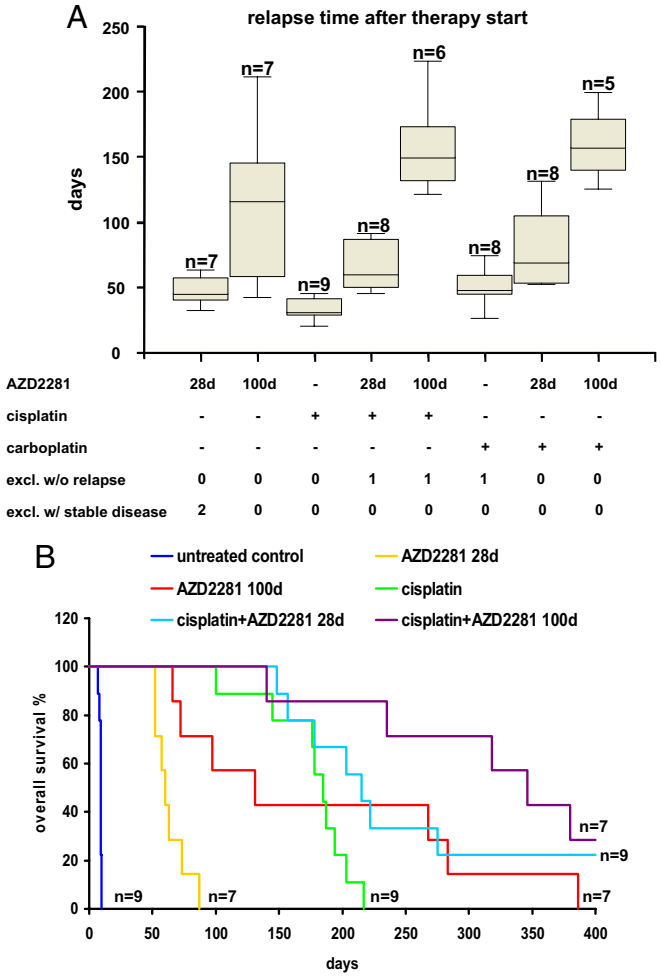

Fig. 5. Combination of AZD2281 with carboplatin and cisplatin prolongs recurrence-free survival and overall survival. (*A*) Box plots indicate the time after therapy start before tumors relapse back to the size when treatment was initiated. Dosing was as follows: 50 mg of AZD2281 per kg i.p. daily for 28 days (28d) or daily for 100 days (100d), 6 mg of cisplatin per kg i.v. on day 0 (30 min after the first AZD2281 injection), 100 mg of carboplatin per kg i.v. on day 0 (30 min after the first AZD2281 injection). (*B*) Kaplan–Meyer curves showing the overall survival after 400 days. Wilcoxon signed rank tests: control vs. AZD2281–28d: $P < 0.009$ ($n = 7$); control vs. AZD2281–100d: $P < 0.009$ ($n = 7$); AZD2281–28d vs. AZD2281–100d: $P < 0.009$ ($n = 7$); cisplatin vs. cisplatin+AZD2281–28d: $P < 0.019$ ($n = 9$); cisplatin vs. cisplatin+AZD2281–100d: $P < 0.014$ ($n = 7$).

drugs against BRCA1-deficient mammary tumors, suggesting this drug combination might be beneficial in the clinic. Additional preclinical studies in the *K14cre;Brca1*$^{F/F}$*;p53*$^{F/F}$ mouse model can be performed to optimize AZD2281-platinum combination therapy, e.g., by applying AZD2281 in combination with multiple low-dose platinum treatments or by applying triple combinations of AZD2281 with tariquidar and platinum drugs. Repeated treatment of animals with cisplatin alone or in combination with AZD2281 resulted in accumulating nephrotoxicity. In the *K14cre;Brca1*$^{F/F}$*;p53*$^{F/F}$ mouse model, different schedules of AZD2281-platinum combinations that maximize tumor cell kill without increasing toxicity can be explored.

As for all new anticancer agents that enter the clinic, one can expect the development of resistance to occur. Using the *K14cre;Brca1*$^{F/F}$*;p53*$^{F/F}$ mammary tumor model, we were able to model acquired resistance to AZD2281 and to investigate the mechanistic basis of this resistance (27). The most frequently observed mechanism of acquired resistance to AZD2281, upregulation of P-gp, could be effectively blocked by the P-gp inhibitor tariquidar, suggesting this might be a suitable strategy to reverse P-gp-related clinical resistance to AZD2281 should it occur. Interestingly, P-gp expression might also be directly modulated by PARP1 inhibition, because mouse embryonic fibroblasts from *Parp1*$^{-/-}$ mice were found to have increased P-gp expression and doxorubicin resistance that could be reversed by the P-gp modulator verapamil (28). To identify alternative P-gp-independent resistance mechanisms, we are currently crossing the *K14cre;Brca1*$^{F/F}$*;p53*$^{F/F}$ model onto an *Abcb1a/b* null background (29). In human *BRCA*-mutated breast cancer, acquired resistance to AZD2281 might also be mediated by genetic reversion of the *BRCA1* or *BRCA2* mutations (30–32). This possibility cannot be investigated in our current mouse model, in which BRCA1 function is irreversibly abolished by Cre-mediated deletion of exons 5–13 (12), disabling the development of platinum resistance by genetic reconstitution of BRCA1 function (13, 33). New mouse models containing *Brca1* frame shift mutations that mimic common human *BRCA1* founder mutations are required to investigate whether such a resistance mechanism does occur in vivo.

Our study shows that GEMMs of human cancer may be useful not only for assessment of tumor response and toxicity but also for modeling acquired resistance, analysis of resistance mechanisms, and evaluation of reversal strategies or second-generation drugs in resistant tumors. Hence, intervention studies in GEMMs may help to predict the basis of resistance to novel therapeutics well in advance of the human experience, thereby providing the possibility to more adequately respond to clinical resistance. Ultimately, this may improve the clinical success rate for novel anticancer drugs.

Materials and Methods

Animals, Generation of Mammary Tumors, and Orthotopic Transplantations. *Brca1*$^{-/-}$*;p53*$^{-/-}$ mammary tumors were generated in *K14cre;Brca1*$^{F/F}$*;p53*$^{F/F}$ mice, genotyped, and orthotopically transplanted into syngeneic wild-type mice as described (12, 13, 34). *Ecad*$^{-/-}$*;p53*$^{-/-}$ mammary tumors were generated in *WAPcre;Ecdh*$^{F/F}$*;p53*$^{F/F}$ mice (P.W.B.D. and J.J., unpublished results) and transplanted as *Brca1*$^{-/-}$*;p53*$^{-/-}$ tumors. Starting 2 weeks after tumor grafting, the onset of tumor growth was checked at least 3 times per week. Mammary tumor size was determined by caliper measurements (length and width in millimeters) and tumor volume (in mm^3) was calculated by using the following formula: $0.5 \times \text{length} \times \text{width}^2$. Animals were killed with CO_2 when the tumor volume reached 1,500 mm^3. In addition to sterile collection of multiple tumor pieces for grafting experiments, tumor samples were snap-frozen in liquid nitrogen and fixed in 4% formaline. All experimental procedures on animals were approved by the Animal Ethics Committee of The Netherlands Cancer Institute.

Drugs. AZD2281 was used by diluting 50 mg/ml stocks in DMSO with 10% 2-hydroxyl-propyl-β-cyclodextrine/PBS such that the final volume administered by i.p. injection was 10 μL/g of body weight. Cisplatin (1 mg/mL in saline-mannitol) and carboplatin (10 mg/mL in mannitol–H_2O) originated from Mayne Pharma. Tariquidar (Avaant) was diluted in 5% glucose such that the final volume administered by i.p. injection was 10 μL/g of body weight.

Treatment of Mammary Tumor-Bearing Animals. When mammary tumors reached a size of ≈200 mm^3, 50 mg/kg AZD2281 was given i.p. daily for 28 or 100 consecutive days. Controls were left untreated or were dosed with vehicle only. Cisplatin (6 mg/kg) and carboplatin (100 mg/kg) were injected i.v. When combined with platinum drugs, AZD2281 was given 30 min in advance. After the initial treatment, the tumor size was determined at least 3 times per week. The relative tumor volume was calculated as the ratio between the tumor volume at time *t* and the tumor volume at the start of treatment. To avoid accumulating toxicity of repeated drug injections, an additional treatment was not given after the recovery time of 14 days when the tumor responded to the treatment (tumor size <50% of the original volume, partial response). In this case, treatment was resumed once the tumor relapsed to its original size (100%).

AZD2281 PK/PD Analysis. Three primary *Brca1*$^{-/-}$;*p53*$^{-/-}$ tumors (T1–T3) were transplanted into 5 animals each, and 4 of these mice were treated with 50 mg of AZD2281 per kg i.p. when the tumor volume reached 500 mm^3. Tumor and plasma samples were harvested 30 min, 2 h, 6 h, and 24 h. The tumor of the fifth animal was used as control when 500 mm^3 in size. Tumors were homogenized for 1 min in 3 volumes of ice-cold PBS and tumor and plasma samples snap frozen on dry-ice. The concentration of AZD2281 was determined by liquid chromatography–tandem mass spectrometry (LC-MS/MS) on an Agilent 1100 series LC system linked to a Sciex 2000 triple Quad Mass Spectrometer (Applied Biosystems). After thawing, the compound was extracted from the sample by protein precipitation with acetonitrile and injected on an acetonitrile (0.01% formic acid): 0.01% formic acid gradient. Calibration standards were prepared in mouse plasma and tumor as proxy matrices. To measure PARP1 activity tumor whole-cell extracts (WCE) were first analyzed by Western blot by using the anti-PARP1 mouse monoclonal 7D3–6 (BD Bioscience) followed by ECL detection and quantitative image analysis (LAS-3000, Fuji/Raytek). The PARP1 protein concentration for each extract was determined by 2D densitometry against PARP1 standards using AIDA (Advanced Image Data Analyzer) imaging software. The equivalent of 20 pg of PARP1 of mouse tumor WCEs were then activated ex vivo by incubating with dsDNA oligos and NAD+ to stimulate PARP1 activity and polyADP-ribosylation (PAR formation). PAR formation was then quantified by electrochemiluminescence with a Meso Scale assay by using the anti-PAR mouse monoclonal 10H (Serotec) primary antibody followed by a goat anti-mouse IgG SULFO-TAG (Meso Scale) secondary antibody.

RT-MLPA Analysis. From the snap-frozen tumor samples total RNA was isolated with TRIzol (Invitrogen) and the integrity of RNA was verified by denaturing gel electrophoresis. Reverse transcription, hybridization, ligation, PCR amplification, and fragment analysis by capillary electrophoresis were performed as described (13, 35).

Immunohistochemical Analysis. Immunohistochemical stainings of tumors were carried out by using anti-γH2AX [rabbit polyclonal, Cell Signaling, #2577, 1:50 in 1% bovine serum albumin diluted in phosphate saline buffer (PBSA)] and anti-cleaved caspase 3 (rabbit polyclonal, Cell Signaling, #9661, 1:100 in 1% PBSA) antibodies. Antigen retrieval was performed by boiling for 15 min in citrate buffer (pH 6.0). After overnight probing at 4 °C with the primary antibodies, slides were incubated with a biotinylated goat anti-rabbit secondary antibody (Dakocytomation, # E043201, 1:800 in 1% PBSA) for 30 min at room temperature. For detection, we used a standard StreptABC amplified staining procedure with DAB (Dakocytomation, # K037711) and haematoxylin counterstaining. Positive and negative (no antibody) controls were included for each slide and staining procedure. Positively labeled cells (in the case of γH2AX ≥1 dot per nucleus) were counted in the tumor sections in 10 standardized microscopic fields (650 × 650 μm). These fields were defined by using an ocular morphometric grid and a 40× lens.

ACKNOWLEDGMENTS. We thank Anton Berns, Maarten van Lohuizen, and Jan Schellens for critical reading of the manuscript and Susan Bates and Tito Fojo from the National Institutes of Health, Bethesda, MD, for providing tariquidar. This work was supported by grants of the Dutch Cancer Society (2002-2635 to J.J. and A. Berns; 2006-3566 to P.B., S.R., and J.J.; 2007-3772 to J.J., S.R., and J. H. M. Schellens), The Netherlands Organization for Scientific Research (NWO-Veni 916.56.135, to P.W.B.D.), and the European Union (FP6 Integrated Project 037665-CHEMORES to P.B. and S.R.). S.R. was supported by fellowships from the Swiss National Science Foundation (PBBEB-104429) and the Swiss Foundation for Grants in Biology and Medicine.

1. de Murcia J, *et al.* (1997) Requirement of poly(ADP-ribose) polymerase in recovery from DNA damage in mice and in cells. *Proc Natl Acad Sci USA* 94:7303–7307.
2. Schreiber V, Dantzer F, Ame JC, de Murcia G (2006) Poly(ADP-ribose): Novel functions for an old molecule. *Nat Rev Mol Cell Biol* 7:517–528.
3. Wang ZQ, *et al.* (1997) PARP is important for genomic stability but dispensable in apoptosis. *Genes Dev* 11:2347–2358.
4. Bryant HE, *et al.* (2005) Specific killing of BRCA2-deficient tumours with inhibitors of poly(ADP-ribose) polymerase. *Nature* 434:913–917.
5. Farmer H, *et al.* (2005) Targeting the DNA repair defect in BRCA mutant cells as a therapeutic strategy. *Nature* 434:917–921.
6. Narod SA, Foulkes WD (2004) BRCA1 and BRCA2: 1994 and beyond. *Nat Rev Cancer* 4:665–676.
7. Gudmundsdottir K, Ashworth A (2006) The roles of BRCA1 and BRCA2 and associated proteins in the maintenance of genomic stability. *Oncogene* 25:5864–5874.
8. Helleday T, *et al.* (2008) DNA repair pathways as targets for cancer therapy. *Nat Rev Cancer* 8:193–204.
9. Donawho CK, *et al.* (2007) ABT-888, an orally active poly(ADP-ribose) polymerase inhibitor that potentiates DNA-damaging agents in preclinical tumor models. *Clin Cancer Res* 13:2728–2737.
10. Sharpless NE, Depinho RA (2006) The mighty mouse: Genetically engineered mouse models in cancer drug development. *Nat Rev Drug Discov* 5:741–754.
11. Menear KA, *et al.* (2008) 4-[3-(4-Cyclopropanecarbonyl-piperazine-1-carbonyl)-4-fluoro-benzyl]-2-H-phthalazin-1-one, a novel bioavailable inhibitor of poly(ADP-ribose) polymerase-1, PARP-1. *J Med Chem*, in press.
12. Liu X, *et al.* (2007) Somatic loss of BRCA1 and p53 in mice induces mammary tumors with features of human BRCA1-mutated basal-like breast cancer. *Proc Natl Acad Sci USA* 104:12111–12116.
13. Rottenberg S, *et al.* (2007) Selective induction of chemotherapy resistance of mammary tumors in a conditional mouse model for hereditary breast cancer. *Proc Natl Acad Sci USA* 104:12117–12122.
14. Derksen P, *et al.* (2006) Somatic inactivation of E-cadherin and p53 in mice leads to metastatic lobular mammary carcinoma through induction of anoikis resistance and angiogenesis. *Cancer Cell* 10:437–449.
15. Raymond M, Rose E, Housman DE, Gros P (1990) Physical mapping, amplification, and overexpression of the mouse mdr gene family in multidrug-resistant cells. *Mol Cell Biol* 10:1642–1651.
16. Allen JD, Brinkhuis RF, Wijnholds J, Schinkel AH (1999) The mouse Bcrp1/Mxr/Abcp gene: Amplification and overexpression in cell lines selected for resistance to topotecan, mitoxantrone, or doxorubicin. *Cancer Res* 59:4237–4241.
17. Mistry P, *et al.* (2001) In vitro and in vivo reversal of P-glycoprotein-mediated multidrug resistance by a novel potent modulator, XR9576. *Cancer Res* 61:749–758.
18. Evers B, *et al.* (2008) Selective inhibition of BRCA2-deficient mammary tumor cell growth by AZD2281 and cisplatin. *Clin Cancer Res* 14:3916–3925.
19. Cleator S, Heller W, Coombes RC (2007) Triple-negative breast cancer: Therapeutic options. *Lancet Oncol* 8:235–244.
20. Sorlie T, *et al.* (2001) Gene expression patterns of breast carcinomas distinguish tumor subclasses with clinical implications. *Proc Natl Acad Sci USA* 98:10869–10874.
21. Foulkes WD, *et al.* (2003) Germline BRCA1 mutations and a basal epithelial phenotype in breast cancer. *J Natl Cancer Inst* 95:1482–1485.
22. Turner N, Tutt A, Ashworth A (2004) Hallmarks of 'BRCAness' in sporadic cancers. *Nat Rev Cancer* 4:814–819.
23. Turner NC, *et al.* (2007) BRCA1 dysfunction in sporadic basal-like breast cancer. *Oncogene* 26:2126–2132.
24. Yap TA, *et al.* (2007) First in human phase I pharmacokinetic (PK) and pharmacodynamic (PD) study of KU-0059436 (Ku), a small molecule inhibitor of poly ADP-ribose polymerase (PARP) in cancer patients (p), including BRCA1/2 mutation carriers. *J Clin Oncol*, ASCO Annual Meeting Proceedings Part I 25:3529.
25. Kelland L (2007) The resurgence of platinum-based cancer chemotherapy. *Nat Rev Cancer* 7:573–584.
26. Flohr C, Bürkle A, Radicella JP, Epe B (2003) Poly(ADP-ribosyl)ation accelerates DNA repair in a pathway dependent on Cockayne syndrome B protein. *Nucleic Acids Res* 31:5332–5337.
27. Rottenberg S, Jonkers J (2008) Modeling therapy resistance in genetically engineered mouse cancer models. *Drug Resist Updat* 11:51–60.
28. Wurzer G, Herceg Z, Wesierska-Gadek J (2000) Increased resistance to anticancer therapy of mouse cells lacking the poly(ADP-ribose) polymerase attributable to upregulation of the multidrug resistance gene product P-glycoprotein. *Cancer Res* 60:4238–4244.
29. Schinkel AH, *et al.* (1997) Normal viability and altered pharmacokinetics in mice lacking mdr1-type (drug-transporting) P-glycoproteins. *Proc Natl Acad Sci USA* 94:4028–4033.
30. Sakai W, *et al.* (2008) Secondary mutations as a mechanism of cisplatin resistance in BRCA2-mutated cancers. *Nature* 451:1116–1120.
31. Swisher EM, *et al.* (2008) Secondary BRCA1 mutations in BRCA1-mutated ovarian carcinomas with platinum resistance. *Cancer Res* 68:2581–2586.
32. Edwards SL, *et al.* (2008) Resistance to therapy caused by intragenic deletion in BRCA2. *Nature* 451:1111–1115.
33. Borst, P., Rottenberg, S. and Jonkers, J (2008) How do real tumors become resistant to cisplatin? *Cell Cycle* 7:1353–1359.
34. Jonkers J, *et al.* (2001) Synergistic tumor suppressor activity of BRCA2 and p53 in a conditional mouse model for breast cancer. *Nat Genet* 29:418–425.
35. Eldering E, *et al.* (2003) Expression profiling via novel multiplex assay allows rapid assessment of gene regulation in defined signalling pathways. *Nucleic Acids Res* 31:e153.